GEOFISICA INTERNACIONAL

REVISTA DE LA UNION GEOFISICA MEXICANA, AUSPICIADA POR EL INSTITUTO DE GEOFISICA DE LA UNIVERSIDAD NACIONAL AUTONOMA DE MEXICO

Vol. 24 México, D. F., 1o. de abril de 1985 Núm.2

VOLCANIC ACTIVITY AND CLIMATES OF THE EARTH AND MARS

K. Ya. KONDRATYEV*
N. I. MOSKALENKO
S. N. PARZHIN
S. Ya. SKVORTSOVA

(Received: January 3, 1985)
(Accepted: February 13, 1985)

RESUMEN

Se considera un impacto climático del volcanismo sobre la Tierra y Marte y se hace su análisis comparativo. Se analiza la influencia de los componentes gaseosos y aerosoles de la nube volcánica en evolución sobre el efecto de invernadero y el clima de la Tierra y Marte. En relación con las variaciones esporádicas de la intensidad de la actividad volcánica tiene lugar una modulación temporal del clima, con períodos calientes y fríos. Se revela un papel importante del SO_2 y de los aerosoles volcánicos en la formación del clima en los procesos de evolución de la Tierra y Marte.

ABSTRACT

A climatic impact of volcanism on the Earth and Mars is considered and its comparative analysis is performed. The influence of gaseous components and of aerosols from the evolving volcanic cloud on the greenhouse effect and climate of the Earth and Mars is analyzed. In connection with sporadic variations in the intensity of volcanic activity, a temporal modulation of climate takes place with warm and cold periods. An important role of SO_2 and volcanic aerosols in formation of climate in the process of evolution of the Earth and Mars is revealed.

* *Voeikov Main Geophysical Observatory, Leningrad, URSS.*

INTRODUCTION

Temporal variations of climates taking place on the Earth and Mars necessitate a search for the causes of these variations. Strong changes of climate on the Earth in its early stage of evolution, the climate change on the Earth in our days, observations testifying to a warmer climate on Mars in the past epochs, a recorded impact of dust storms on the radiative regime and climates on the Earth and Mars, all this testifies to the existence of internal factors affecting the radiative regime and climate of the planets. The analysis of these factors was made by Kondratyev and Moskalenko (1977, 1983), Kondratyev and Hunt (1981), and by others. The factors mentioned above include, in particular, changes in the gas and aerosol composition of the atmospheres. The gas composition of atmospheres varies smoothly, according to the laws of nature, due to outgassing of the solid shell of the planet and biochemical processes taking place in the atmosphere and on the planetary surface, while changes in the aerosol composition and aerosol optical properties are often sporadic, which causes strong changes in climate. The volcanic activity, whose climatic impact on the Earth and on Mars has exhibited substantial temporal fluctuations due to temporal variations in the intensity of the volcanic activity, is one of the powerful factors which cause planetary-scale climate changes.

Powerful volcanic ejections not only change the aerosol composition of the atmosphere but also its gas composition. Note should be taken of the fact that with the intensification of the volcanic activity the amount of SO_2 injected to the stratosphere and troposphere grows. SO_2 is known to have strong absorption bands in the UV and IR spectral regions, shown in Figs. 1, 2. Consequently, an increase in the SO_2 concentration decreases the planetary albedo, enlarges the shortwave radiation absorbed by the planet, and raises the effective temperature of the planet. Strong IR SO_2 bands lead to the intensification of the radiative cooling of the troposphere and to the enhancement of the greenhouse effect near the surface.

Being injected to the stratosphere, the volcanic aerosol further evolves due to photochemical and gas-to-particle conversion of SO_2. The H_2SO_4-solution aerosol resulting from this conversion brings forth substantial changes in the content and optical properties of the stratospheric aerosol: a decreased absorption of the shortwave radiation by aerosols, and

an increased aerosol activity in the longwave spectral region. The process of formation of sulphate aerosols is followed by a decrease in the SO_2 concentration. This results in an increase in the planetary albedo and a decrease in the surface temperature.

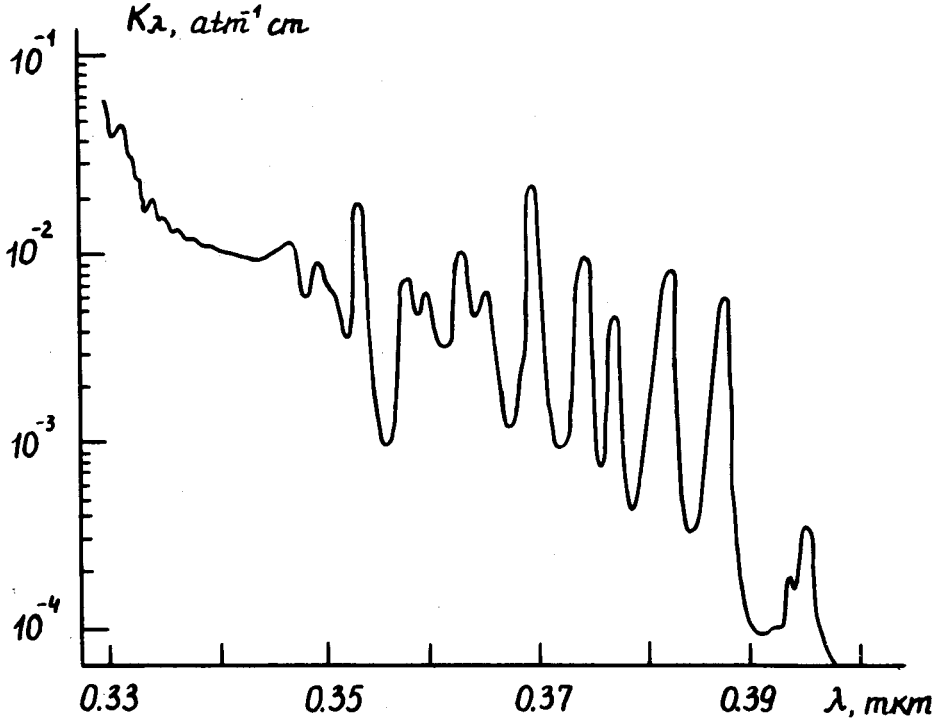

Fig. 1. The spectral dependence of the SO_2 absorption coefficient in the spectral intervals 0.3 - 0.4 μm.

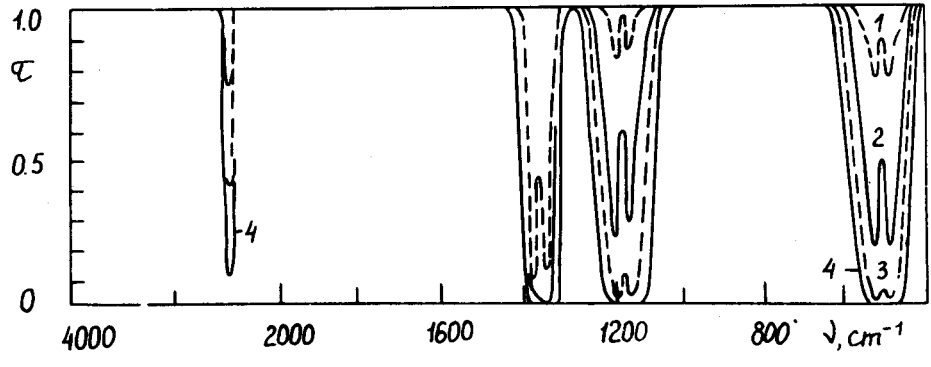

Fig. 2. SO_2 absorption spectra for the contents, ω, atm.cm: 1-0.15; 2-1.2; 3-5; 4-10.

During the Earth's evolution the optical thickness of the stratospheric aerosol layer has changed considerably. According to calculations by Kondratyev and Moskalenko (1980), the optical thickness of the stratospheric aerosol during maximum volcanic activity reached $\tau = 4.4$. At present, a temporal change of volcanic activity takes place, which causes variations in the radiative regime of the atmosphere and climate.

MODELLING THE OPTICAL PROPERTIES OF AN EVOLVING ATMOSPHERE

The major impact of the atmosphere on the planetary radiative regime is connected with the mechanism of the greenhouse effect, which causes the warming of the surface and of the troposphere. The impact of the atmospheric greenhouse effect was calculated using a 1-D radiative-convective climate model based on radiation parameterization suggested by Kondratyev and Moskalenko (1980), with account of radiation absorption by all important atmospheric gases, the absorbing and scattering properties of cloudiness, as well as the tropospheric and stratospheric aerosols. The spectral transmission functions (STF) of gas components were calculated with the use of programmes and STF parameterization after Moskalenko *et al.* (1969, 1971, 1978), based on data of complex experiments and STF line-by-line calculations performed by Moskalenko and Yakupova (1978). The absorption in the 0.1 - 100μm spectral interval by H_2O, CO_2, O_3, N_2O, CH_4, NO, CO, O_2, N_2, NO_2, NH_3, OH, HCl, was taken into account. In calculations was also used an *a-priori* information about the chemical composition of atmospheres discussed in monographs by Kondratyev and Moskalenko (1977), by Moroz (1978), and by Marov (1981). When necessary, the information was supplemented by respective calculation data, based on consideration of the sources and sinks of gas and aerosol components, described by Kondratyev, Moskalenko, Pozdnyakov (1983).

The aerosol component of the atmospheres was simulated by superimposing the gamma-distributions, in accordance with studies by Kondratyev, Moskalenko, Terzi (1981), the optical characteristics of which (the coefficients of absorption and scattering, the phase functions) have been obtained with due regard to the actual chemical composition of aerosols. The representation of atmospheric aerosols and clouds as a superposition of different fractions, each having its vertical profile, size distribution and chemical composition, makes it possible to realistically consider the vertical inhomogeneity of aerosols and clouds. A bank of

optical characteristics, including about 50 types of aerosols and clouds, enables one to simulate a spatial variability of the optical characteristics of the aerosol component, with the atmospheric aerosol and clouds considered as a joint scattering and absorbing medium. The use of the above mentioned data bank permits the simulation of the aerosol components of atmospheres in the process of their evolution. Figure 3 exemplifies the spectral dependences of the attenuation coefficient, $\sigma_{a,\lambda}$, as well as absorption coefficient, $\sigma^a_{a,\lambda}$ for different fractions of the volcanic aerosol. The $\sigma^a_{a,\lambda}$ and $\sigma_{a,\lambda}$ values were normalized against $\sigma_{a,\lambda}$ at $\lambda = 0.5\,\mu m$. Figure 3 illustrates spectral variations of the absorbing and scattering properties of volcanic aerosols, when their size distribution changes.

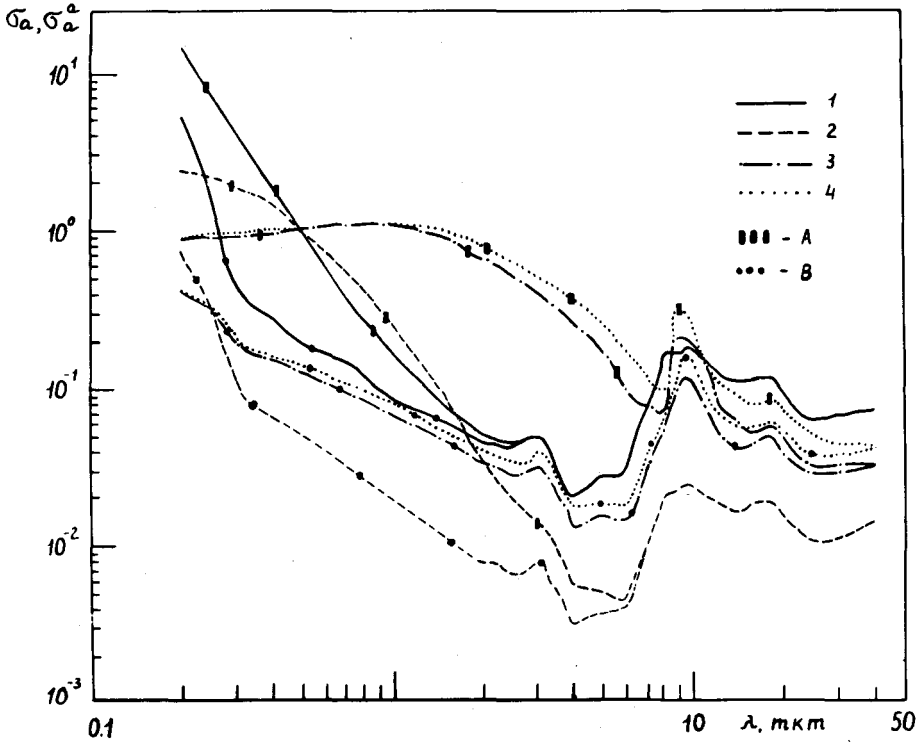

Fig. 3. The spectral dependence of the coefficients of attenuation, σ_a, (A) and absorption, σ^a_a(B) for different fractions of the volcanic aerosol. The size distribution of the ensemble of spherical particles is described with the gamma distribution for the following parameters:

1 - a = 1; b = 50; c = 0.5
2 - a = 1; b = 25; c = 0.5
3 - a = 1; b = 12.5; c = 0.5
4 - a = 1; b = 9; c = 0.5

The chemical composition and structural characteristics of an evolving atmosphere substantially change in time, and, therefore, it is important to take into account the effect of these changes on the optical properties of the gas and aerosol components of the atmosphere. Techniques for calculation of the atmospheric absorption with due regard to selective absorption in the rotational-vibrational bands, to the continuum absorption by far wings of lines, and to the pressure-induced absorption, are described in monographs by Kondratyev and Moskalenko (1977, 1983). The authors used both the empirical spectral transmission functions and the STF calculated with the help of the line-by-line technique based on parameters after MacClatchey (1973), Kayumova *et al.* (1979), Moskalenko and Zotov (1977), Moskalenko and Yakupova (1978). The application of various techniques for STF calculation to the thermal emission transfer in absorbing and scattering media has been discussed by Moskalenko and Zakirova (1972), Kondratyev and Moskalenko (1977). In STF calculations their temperature dependence has been considered both in rotational and vibrational bands and in pressure-induced absorption bands.

An importance of consideration of the temperature effect on the STF is exemplified in Figs. 4 and 5 by the absorption bands for carbon dioxide and ozone.

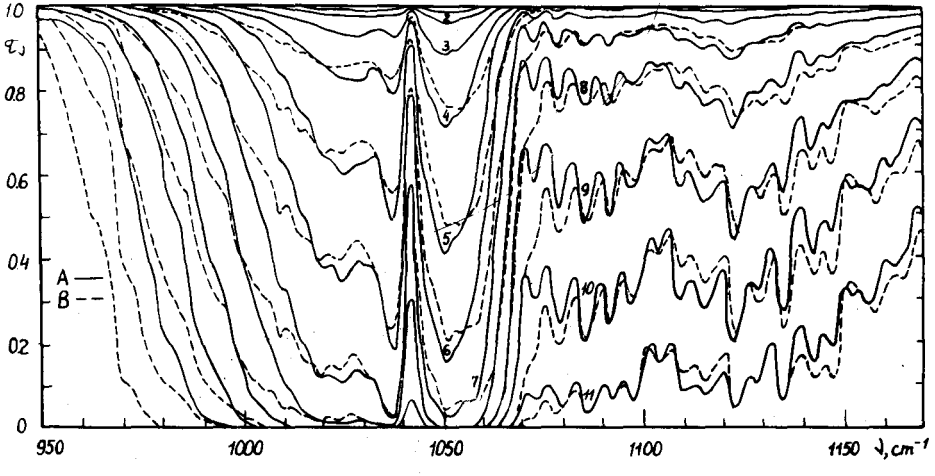

Fig. 4. Transmission spectra in the 9.6 μm O_3 band at t = 200K (A) and 300K (B). the content, ω, atm.cm: 1-0.001; 2-0.003; 3-0.01; 4-0.03; 5-0; 6-0.3; 7-1; 8-3; 9-10; 10-30; 11-100. Nitrogen-broadening at a pressure of P_{N_2} = 0.1 atm.

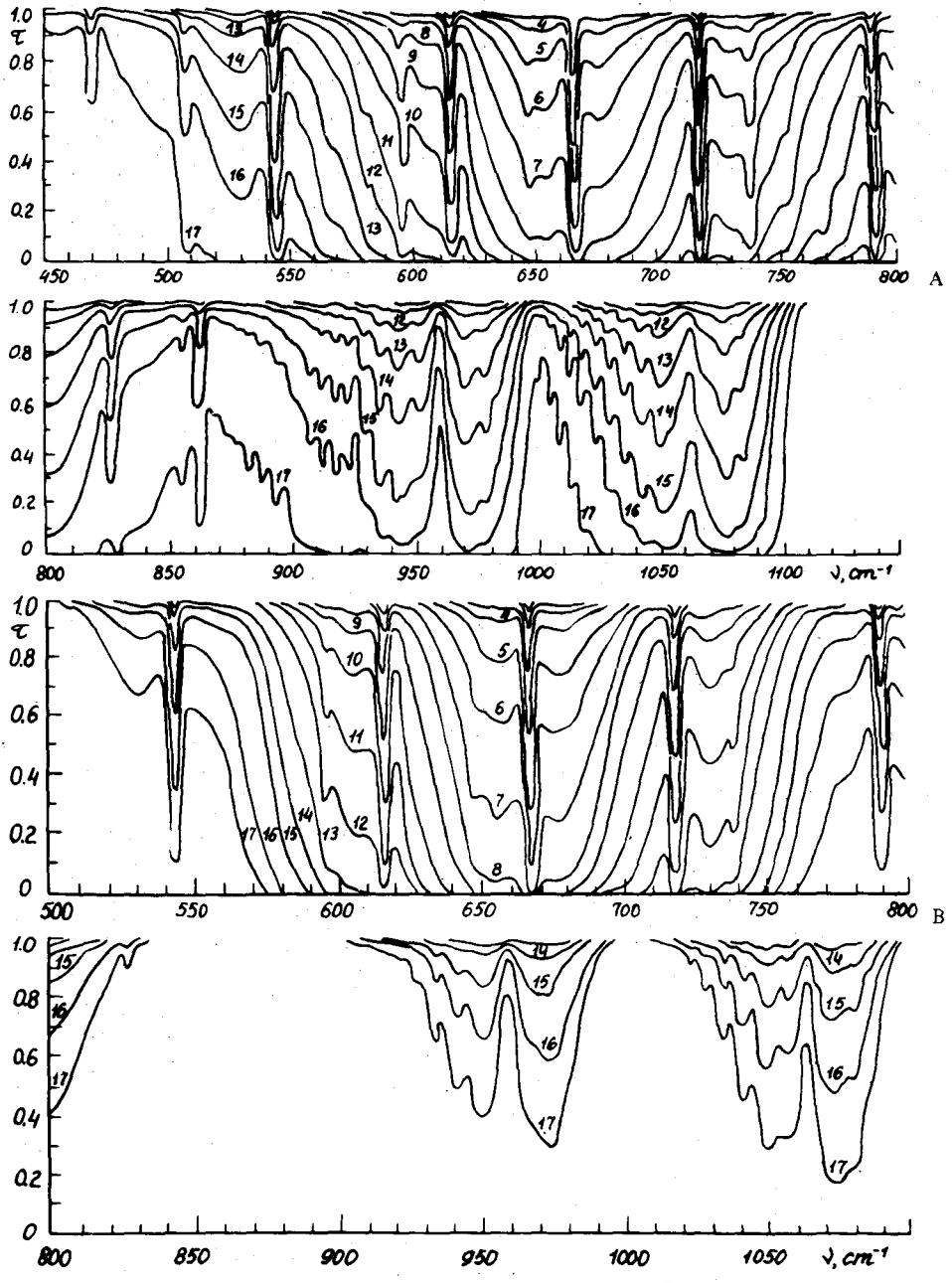

Fig. 5. Spectral transmission functions for nitrogen-broadened CO_2 at t = 300K (A) and 200K (B) and P_{N_2}= 1 atm.
ωCO_2, atm.cm: 1-0.001; 2-0.003; 3-0.01; 4-0.03; 5-0.1; 6-0.3; 7-1; 8-3; 9-10; 10-30; 11-100; 12-300; 13-1000; 14-3000; 15-10 000; 16-30 000; 17-300 000.

The construction of the models of clouds and atmospheric haze is based on the following assumptions: aerosols and clouds have a multimodal size distribution and are represented by an equivalent ensemble of homogeneous spherical particles. The size distribution $N_i(r)$ for each fraction of a given chemical composition was described in our studies by the gamma function. Then the number density

$$N(r) = \sum_{i=1}^{N} N_i(r) = \sum_{i=1}^{N} A_i(z) r^{a_i} \exp(-b_i r^{c_i}) \qquad (1)$$

where $A_i(z)$ depends on height (z); a_i, b_i, c_i are the parameters of the i-th fraction. Fractions $N_i(r)$ can be represented by the particles of clouds of aerosols (located both below and above clouds).

In connection with the fact that most reliable information on the vertical structure of aerosols and clouds has been obtained from the optical density data (at $\lambda = 0.55\,\mu m$), the values of the scattering coefficients, $\sigma^{s}_{a,\lambda}$, and absorption coefficients $\sigma^{a}_{a,\lambda}$, are normalized against the optical density. In the atmosphere

$$(\sigma^{a,s}_{a,\lambda}(Z) = \sum_{i=1}^{N} B_i(Z)\, \sigma^{a,s}_{a,\lambda_i} \qquad (2)$$

$$f_\lambda(Z,\theta) = \sum_{i=1}^{N} B_i(Z) f_{\lambda_i} / \sum_{i=1}^{N} B_i(Z) \qquad (3)$$

where $B_i(z)$ is the optical density vertical profile for the i-th fraction of either aerosols or cloudiness (the attenuation coefficient at $\lambda = 0.55\,\mu m$).

The models of aerosols and clouds were computed using the programme of an aerosol block. The optical characteristics of the aerosol component for different fractions (1) were obtained from calculations based on Mie theory described by Deirmendjian (1971) for different types of aerosol formations of the atmospheres of the Earth and Mars.

To solve the problems of the temperature regimes of the atmospheres, it is necessary to assess the vertical profiles of radiative flux divergences of the shortwave and longwave radiation. For this purpose the phase function is calculated both for the parallel and perpendicular polarization of the electromagnetic components:

$$f_\lambda(\psi) = [f_{\lambda\perp}(\psi) + f_{\lambda\parallel}(\psi)]/2 \qquad (4)$$

The suggested models of the aerosol components of the planetary atmospheres make it possible to construct global zonal optical models of atmospheric aerosols. The same conclusion is true for the chemical composition and size distribution of cloud particles. If necessary, the consideration of the optical properties of the aerosol components of planets enables one to model a 3-D field of distribution of the optical characteristics of the planetary aerosol components.

In calculations of the STF of the gas phase of the atmosphere it is necessary to separate the contributions to the absorption from the wings of distant spectral lines for atmospheric gases, $\tau^{c}_{\Delta\gamma}$, from the pressure-induced absorption, $\tau^{i}_{\Delta\gamma}$, and from the selective absorption, $\tau^{s}_{\Delta\gamma}$, of spectral absorption lines, within a given spectral interval. This division makes it possible to substantially raise the accuracy of calculation of $\tau_{\Delta\gamma}$ and to broaden the confidence interval for the content of the absorbing gas, for pressure, and for temperature. Then, for the given component

$$\tau_{\Delta\gamma} = \tau^{c}_{\Delta\gamma} \cdot \tau^{i}_{\Delta\gamma} \cdot \tau^{s}_{\Delta\gamma} \tag{5}$$

the function.

$$\tau^{c}_{\Delta\gamma} \cdot \tau^{i}_{\Delta\gamma} = \exp[-\beta_{\gamma c}(T) + \beta_{\gamma i}(T)\omega P] \tag{6}$$

The calculation of $\tau^{s}_{\Delta\gamma}$ using an empirical technique proposed by Moskalenko *et al.* (1972) is based on the following equation:

$$\left(\frac{1}{\ell_n \tau^{s}_{\Delta\gamma}}\right)^2 = \left(\frac{1}{\ell_n \tau'^{s}_{\Delta\gamma}}\right)^2 + \left(\frac{1}{\ell_n \tau''^{s}_{\Delta\lambda}}\right)^2 + \frac{M}{(\ell_n \tau'^{s}_{\Delta\gamma})(\ell_n \tau''^{s}_{\Delta\gamma})} \tag{7}$$

where

$$\tau'^{s}_{\Delta\gamma} = \exp[-K_{\gamma}(T)\omega] \,, \tag{8}$$

$$\tau''^{s}_{\Delta\gamma} = \exp[-\beta_{\gamma s}(T)\omega^{m\gamma} P_e^{n\gamma}] \tag{9}$$

$\tau'^{s}_{\Delta\gamma}$ determines the STF at high pressures in conditions of a smeared rotational structure; $\tau''^{s}_{\Delta\gamma}$ is a satisfactory STF approximation for the region of strong absorption. The parameter M in (7) characterizes a change in the rate of the STF growth in the transition from the region of weak absorption to that of strong absorption. An approximation of strong absorption can be expressed, for instance, as the product of functions:

$$\tau''^{s}_{\Delta\gamma} = \exp[-\beta'_{\gamma s}(T)\omega^{m\gamma} P_e^{n\gamma}][1 - \phi(\beta''_{\gamma s}\omega^{m\gamma} P_e^{n\gamma})] \tag{10}$$

of the logarithmic or any other dependence on $\omega^{m\gamma}P_e^{n\gamma}$.

$\tau^s_{\Delta\gamma}$ along the path, 1, in conditions of an inhomogeneous atmosphere as to temperature, T(1), and pressure, is calculated using the formulae

$$-\ell_n(\tau^s_{\Delta\gamma}) = K_{\gamma s}(T_0)W_{1i} - \ell_n\tau^{ns}_{\Delta\gamma} = \beta_\gamma(T)W_2 \qquad (11)$$

where

$$W_1 = \int_\ell \rho(\ell)F_{1s}[\ell(T)]d\ell \quad , \qquad (12)$$

$$W_2 = \int_\ell \rho(\ell)\left(\frac{P(\ell)}{P_0}\right)^{n\gamma/m\gamma}[\ell(T)]d\ell \quad , \qquad (13)$$

$$F_{1s}(T) = K_\gamma(T)/K_\gamma(T_0) \; ; \qquad F_{2s}(T) = \beta_{\gamma s}(T)/\beta_{\gamma s}(T_0) \qquad (14)$$

Similarly, for the pressure-induced and continuum absorptions

$$\beta_{\gamma i} = \beta_{\gamma i}(T_0)F_i(T) \; ; \qquad \beta_{\gamma c}(T) = \beta_{\gamma c}(T_0)\cdot F_c(T) \qquad (15)$$

The best adaptation of parameters in the above given formulae leads to errors $\Delta\tau = 3\text{-}4\%$, which do not exceed the errors in STF measurements. With the use of accurate STF data obtained through line-by-line calculations, the adaptation to approximations (5) - (10) gave errors $\Delta\tau^s_{\Delta\gamma} = 2\text{-}3\%$.

Calculations of STF for the rectangular and arbitrary instrument function $\delta(\nu - \nu')$ in an inhomogeneous (by temperature and pressure) atmosphere are made using the formulae

$$\tau_{\Delta\gamma} = \frac{1}{\Delta\gamma}\int_\Delta d_\gamma\tau_\gamma(\rho_j(\bar{L})_|\, T(\bar{L}), \bar{L})_| \qquad (16)$$

$$\tau_{\delta\gamma} = \int_\delta d'_{\nu'}\tau_\gamma\delta(\nu - \gamma') \quad , \qquad (17)$$

where

$$\tau_\gamma[\rho_j(L),\ T(L), \bar{L}] =$$

$$= \exp\Big[-\Big\{\frac{\rho}{\bar{L}}\alpha\bar{L}\sum_{ij}S_{ij}\Big\{T(\bar{L}), b_{ij}[P_j(\bar{L}), T(\bar{L}), \bar{L}, \nu_{ij}, \nu]\Big\}\rho_j(\bar{L}) +$$

$$+ \frac{\rho}{\bar{L}}\alpha L\sum_j K^{i,c}_{\nu,i}[P_j(\bar{L}, T(\bar{L})]\Big\}\Big] \qquad (18)$$

where $\rho_j^{\bar{L}}$ is the concentration; $k^{i,c}_{\nu,j}$ are the spectral absorption coefficients determined by molecular interaction; S_{ij}, b_{ij}, ν_{ij} are the intensity, the shape and the center of the i-th line of the j-component. The

length of the optical path for a spherical planet

$$\alpha\bar{L} = dZ/\left\{1-\left[\frac{(R+Z_1)n(Z_1)}{(R+Z)n(Z)}\,\mathrm{Sin}\theta(Z_1)\right]^2\right\}^{1/2} \qquad (19)$$

where z is the height; n(z) is the refractive index; $\theta(z_1)$ is the zenith viewing angle at a height z_1; R is the radius of the planet. In a general case $d\bar{L}$ is given in a numerical form. The temperature dependence of S_{ij} and d_{ij} is determined from the formulae known in spectroscopy. Moskalenko and Yakupova (1978) developed an economical algorithm to compute $\tau_{\Delta,\delta,\nu}$, with due regard to the empirical shape of spectral lines, Foygt's shape and Lorenzian shape. They also calculated the STF's using line-by-line techniques for various absorption bands for water vapour, CO_2, N_2O, NO, CH_4, CO, HCl for a broad range of conditions existing in the atmosphere.

CLIMATIC IMPLICATIONS OF THE VOLCANIC ACTIVITY IN THE PROCESS OF THE EARTH'S EVOLUTION

Let us consider new results from studies of the impact of volcanic eruptions on the atmospheric greenhouse effect and on climate, bearing in mind the earlier results on the evolution of the Earth's greenhouse effect, obtained by Kondratyev and Moskalenko (1979, 1980, 1981, 1983). It is of interest to consider the impact of volcanic activity on the greenhouse effect of the Earth's primordial atmosphere formed about 4.5 billion years ago. Let us assume that the sun irradiance in that period had constituted 75% of that of today. We assume the chemical composition of the initial atmosphere according to Hart's recommendations (1978), *i.e.* the atmosphere of volcanic origin includes 84.2% water, 14.29% CO_2, 1.06% methane, and 0.23% nitrogen. The latter means that the Earth's initial atmosphere was composed mainly of carbon dioxide. The real water vapour concentration in the atmosphere was limited by ambient temperature and grew as the atmospheric pressure and tropospheric temperature increased.

Upon an intensive capture of the dust cloud by the planet, its surface rapidly cooled due to low heat conductivity of soil and low density of the gas shell enveloping the planet. An intensive formation of the Earth's primordial atmosphere first of all had been caused by tectonic and volcanic activities. Most likely the ejected gas contained SO_2 and COS with the total concentration not exceeding 0.1%. This estimate of the concentration of the sulphur-containing components was obtained from

data on the chemical composition of the present day volcanic gases. The mean planetary surface albedo was assumed to be 0.2, bearing in mind that the soil surface in that period had been weakly eroded.

Despite their relatively low concentration, the greenhouse effect of SO_2 and COS may turn out to be rather strong in connection with the shift of the absorption bands with respect to the atmospheric CO_2 bands. Of particular importance is the consideration of the greenhouse effect of SO_2 and COS at low atmospheric temperatures, when the concentration of the atmospheric water vapour is low, and the greenhouse contribution of such volatile atmospheric components as CO_2, CH_4, SO_2, COS becomes more important. At low pressures and temperatures the life time of SO_2 is rather long (it may be a year and longer), and an equilibrium concentration of SO_2 becomes sufficient to produce a considerable greenhouse effect.

A model of the radiative-convective equilibrium was used. The ratio between the adiabatic and the radiative-convective temperature gradients was assumed to be constant during the formation of the primary atmosphere when the atmospheric pressure, P_s, had changed from 0.005 to 0.4 atm. The vertical profiles of pressure P(z) and H_2O concentration $C_{H_2O}(z)$ were calculated. The relative atmospheric humidity r = 56% was assumed to be constant from the surface level to the height of the tropopause, above which the volume concentration of water vapour was assumed to be constant and corresponding to that in the zone of the stratospheric trap.

The presence of SO_2 in the Earth's initial atmosphere had caused an increase in the stratospheric temperature in the altitude range 30-40 km due to absorption of the solar UV radiation. A heating of the troposphere had been caused by the absorption bands of methane, carbon dioxide and water vapour located in the visible and near IR spectral regions. The presence of even small amounts of SO_2 in the atmosphere had protected the planetary surface from the harmful effect of the shortwave UV radiation.

CS_2 and H_2S are also sulphur-containing components to be mentioned. The greenhouse effect of CS_2 is manifested at the expense of the absorption band 1535 cm^{-1} overlapped by water vapour absorption bands. Unfortunately, there is no information about the CS_2 concen-

tration in the products of volcanic eruptions. A great amount of erupted H_2S does not directly affect the optical properties of the atmosphere, the greenhouse effect, and the planetary surface temperature, because of a short life-time of H_2S in the atmosphere.

Carbon monoxide, CO, released in the process of the planets outgassing had a weak greenhouse effect due to absorption in the 4.7 μm band. Hydrochloric acid, HCl, and hydrofluoric acid, HF, do not have absorption bands in the far IR spectral region. The HCl band is centered at 2866.04 cm^{-1} and the band of the first overtone is located near 5868.6 cm^{-1}. The intensities of the HCl bands 0-1 and 0-2 are, respectively, 132 and 3.73 $atm^{-1}cm^{-2}$. A HF molecule has the basic band 0-1 centered at 3961.3 cm^{-1} and the first overtone at 7750.83 cm^{-1}. In connection with the absence of absorption bands in the far IR spectral region, both HCl and HF do not practically affect the greenhouse effect of the atmosphere, but heat it at the expense of solar radiation absorption.

During the volcanic activity the transport of the products of nitrogen compounds into the stratosphere is observed. NO is the most stable compound, but the main greenhouse effect is manifested by other nitrogen oxides: N_2O, N_2O_5, NO_2, and N_2O_4. N_2O has numerous bands covering a spectral region from 0.1 to 20 μm. Detailed studies of N_2O absorption were carried out by Moskalenko and Parzhi (1980), with the N_2O content from fractions of mm to 2.10^4 atm.cm. Intensities of most of the H_2O absorption bands were measured and the STF was parameterized. At present concentrations of N_2O, the greenhouse effect is mainly observed at the expense of absorption bands 7.8; 8.6; 4.54; 4.0, and 3.86 μm.

In laboratory conditions both NO_2 and N_2O_4 are observed simultaneously. A number of NO_2 and N_2O_4 bands are overlapped and their analysis becomes possible due to a decrease in the N_2O_4 concentration taking place when the temperature grows and the $(NO_2+H_2O_4)$ pressure is reduced in the cell. These measurements allowed us to determine independent contributions to the absorption from NO_2 and N_2O_4, and to parameterize their spectral transmission functions. Note that the NO_2 greenhouse effect is mainly determined by absorption in the 6 μm band. However, at the expense of solar shortwave radiation absorption in the interval 0.3-0.6 μm, the climatic impact of NO_2 is quite substan-

tial. Figure 6 exemplifies the NO_2 STF measured in the shortwave spectral region. An increased NO_2 concentration causes a decrease in the planetary albedo and the warming of the upper stratosphere. Due to specific vertical temperature profile an increase in the NO_2 concentration causes a weak anti-greenhouse effect at the expense of growing intensity of the outgoing thermal emission in the 6 μm NO_2 band.

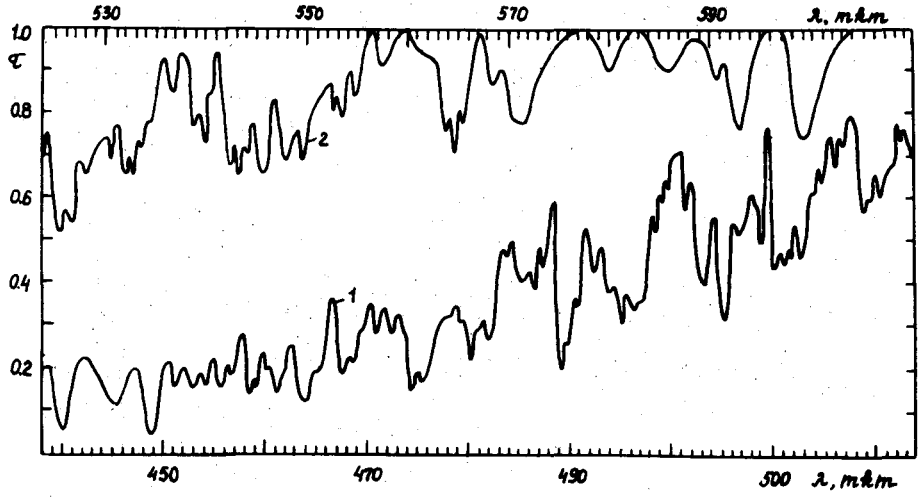

Fig. 6. The NO_2 transmission function in the interval 0.3-0.6 μm at ω = 0.1 atm.cm.

A detailed analysis of the effect of nitrogen oxides on the Earth's climate in the process of the volcanic cloud evolution in the stratosphere requires now unavailable reliable measurements of NO and NO_2 concentrations in the gas products of volcanic eruptions.

Note the importance of considering N_2O_5 and HNO_3 in the radiative heat exchange. The most probable model of the N_2O_5 structure is O_2NONO_2. Strong bands for N_2O_5 are centered at 1720, 1246, 743, and 557 cm^{-1}, and the respective intensities are 1650, 654, 770, and 290 $atm^{-1}cm^{-2}$. Nitric acid vapours have strong absorption bands near 20, 11.2, 7.2, 5.6, and 2.9 μm. Even if their concentration in the atmosphere is not high, they may cause a marked greenhouse effect.

To solve the problem of radiative heat exchange in the Earth's primordial atmosphere, it is important to know the chemical composition of hydrocarbons. An analysis of available measurement data shows that

methane is a prevailing component and constitutes 97-99% of the total content of hydrocarbons. The portion of other hydrocarbons (C_2H_2, C_2H_4, C_2H_6, C_3H_8) is 1-3%. However, at a high concentration of hydrocarbons in the atmosphere, constituting more than 1% by volume, minor hydrocarbons C_2H_2, C_2H_4, C_2H_6, C_3H_8 with strong absorption bands produce a strong greenhouse effect. Detailed studies of hydrocarbons absorption spectra were performed by Moskalenko and Parzhin (1980). The greenhouse effect of hydrocarbons was calculated on the assumption of their constant volume concentration in the primordial atmosphere.

In high layers of the Earth's initial atmosphere hydrogen cyanide (HCN) could have been formed as a result of photolysis which had produced a strong impact on the atmospheric greenhouse effect due to longwave radiation absorption in strong HCN bands 712 and 1412 cm^{-1}.

During volcanic eruptions into a rarefied atmosphere the volcanic tail has reached high altitudes up to 100 km, and the resulting atmospheric aerosol had encircled the planet with a thick layer, whose geometric thickness had diminished with growing density of the atmosphere. With the pressure of the initial atmosphere P_s = 0.4 atm. the aerosol layer had been located within the altitude range 20-30 km.

An effective temperature of the planet is determined by its total albedo, which depends on the chemical composition of the atmosphere, its density, the vertical distribution of the aerosol and cloud components, and on the surface albedo. Figure 7 shows the albedo as a function of the optical thickness for the submicron aerosol fraction, for different surface albedo values, as well as the quantum survival probability for single scattering.

According to our calculations, the mean-planetary surface albedo was assumed to be 0.2 and to be constant in the initial atmospheric pressure range P_s 0.4 atm. As follows from Fig. 7, and from data on the optical characteristics of the stratospheric aerosol (see Fig. 3 and data of Kondratyev, Moskalenko, Pozdnyakov (1983)), the presence of the stratospheric aerosol layer always leads to an increase in the albedo of the surface-atmosphere system (δ) for large optical thickness of aerosol $\tau \approx 0.38$, if the quantum survival probability is 0.9 . With the absorb-

ing gas phase present, the effect of aerosols on the planetary albedo will be weaker.

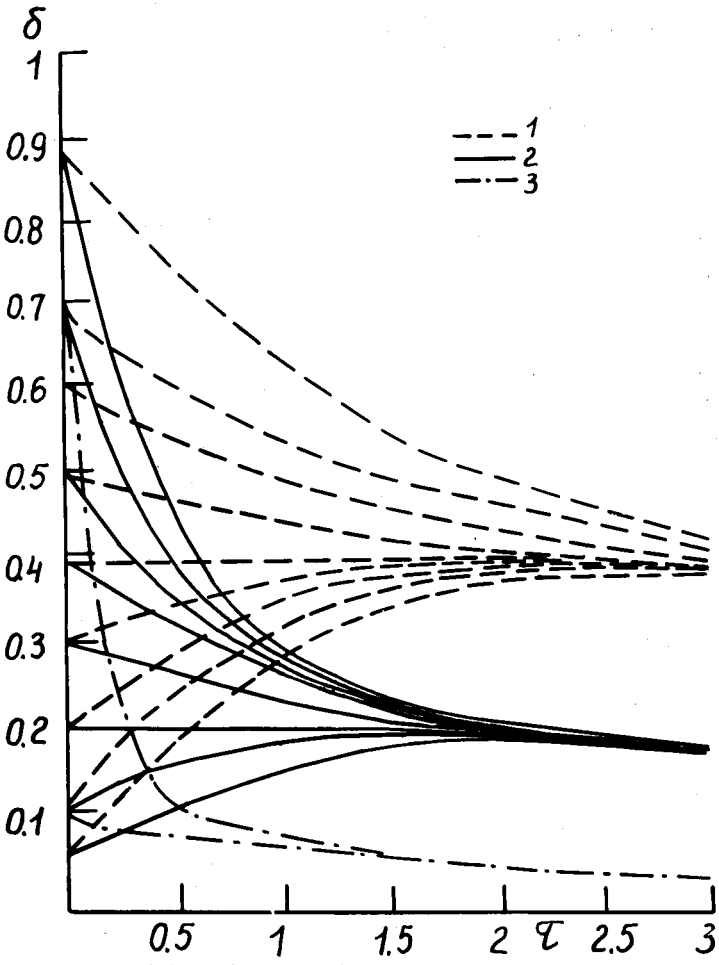

Fig. 7. The dependence of the surface-atmospheric aerosol layer system albedo, δ, on the optical thickness, τ, of an aerosol cloud for stratospheric aerosol models (1), for industrial aerosol (2), and for strongly absorbing aerosol (3) at different surface albedo values, $\delta_S = \delta(\tau = 0)$.

In conditions of intensive volcanic activity the water vapour had been ejected at high altitudes and had photodissociated giving OH, which had caused the absorption of solar radiation by a system of strong bands $A^2\Sigma - X^2\Pi(0,0)$ near $\lambda = 0.31\,\mu m$. Vertical NH_3 profiles were calculated according to Morss and Kuhn (1978). The impact of NH_3 on the greenhouse effect is very strong, and even a small NH_3 concentration in the primordial atmosphere had considerable affected the planetary albedo, causing thereby a warming of the troposphere, an

intensification of the greenhouse effect, and a rise in the planetary surface temperature.

Values of the mean global planetary surface temperature (T_s) as a function of pressure (P_{CO_2}) of the Earth's primordial atmosphere are listed in Table 1. An internal heat source is assumed to be absent, and the vertical optical thickness of the gas-dust cloud in its initial state to be about 0.01.

Table 1

The greenhouse effect of the Earth's primordial atmosphere in the absence of an internal heat source

$P_s(CO_2)$	0.001	0.005	0.01	0.03	0.1	0.2	0.4
δ	0.2	0.203	0.207	0.22	0.26	0.32	0.45
T_e	231	231	230.6	230	227	224	219
T_s	232	237	241	255	270	284	302
T	1	6	10.4	25	43	60	83

The resulting stratospheric aerosol in the altitude range 20-100 km represents a superposition of the small-sized fraction of the volcanic aerosol and the sub-micron fraction of the sulfate aerosol. The large-sized fraction falls out due to sedimentation and is characterized by a short life-time. For the same reason, the large-sized aerosol fraction does not substantially influence the greenhouse effect.

An increase in the planetary albedo (δ) taking place with increasing atmospheric density, is caused by molecular scattering and by growing optical thickness of the stratospheric aerosol layer encircling the planet. Comparisons of results with previous calculations made by Kondratyev and Moskalenko (1979, 1980) without account of absorption by minor components, suggest the conclusion that an account of the effect of minor components in the Earth's initial atmosphere leads to a mean global surface temperature increase by 6K. However, the global greenhouse effect determined by a temperature difference $\Delta T = T_s - T_e$ (T_e is the effective mean global radiative temperature of the planet) is increased by 20K, half the value of the greenhouse effect being caused by the feed-back of an increase in the atmospheric water vapour content when the tropospheric temperature grows due to the greenhouse effect of the atmospheric minor components.

During the formation of the primordial atmosphere the volcanic activity had not still reached its maximum. An intensive formation of craters on the Earth had taken place about 4.3 billion years ago. Calculations showed that during maximum volcanic activity about 4 billion years ago the optical thickness of the stratospheric cloud cover had reached 4.4 .

In the Archaean period the effect of sulphur-containing components on the Earth's climate had been less manifested due to strong opacity of the atmosphere, created by CH_4, NH_3, CO_2 and by water vapour. Therefore, we shall consider specific features of the radiative heat exchange in the volcanically disturbed atmosphere in the anthropogenic period, when the temporal variation of the volcanic activity could have become the major factor of climatic variations.

In the present day atmosphere an intensification of volcanic activity leads to a decrease of the tropospheric temperature and an increase of the stratospheric temperature. The latter is partially caused by the shortwave radiation absorption by SO_2 and by stratospheric aerosols, and mainly by the absorption of the thermal emission from the surface and troposphere by the stratospheric sulfate aerosol.

In the initial stage of an explosive volcanic eruption, rather a sharp warming is observed, which, as the volcanic cloud ejected to the stratosphere evolves, is followed by a slow temporal trend of cooling. The stratospheric aerosol layer with an optical thickness $\tau_a = 0.3$ leads to an increase of the Earth albedo by about 7%, an increase of the stratospheric temperature by about 6K, a decrease of the global radiation by 10%, of the shortwave absorbed radiation by 7%, and a decrease of the global surface temperature by 3-7K (depending on the manifestation of the accompanying feed-backs).

The consideration of the volcanic activity impact on the radiative heat exchange in the Earth's atmosphere suggests the cooling of the surface and of the troposphere. The present day volcanic activity increases a moisture exchange in the oceans-continents-atmosphere system, favouring the accumulation of ice and the broadening of the ice-covered areas. The consideration of different feed-backs in modelling the climatic impact of the volcanic activity is a problem of vital importance.

The climatic impact of the volcanic activity depends on its intensity. With the volcanic activity sufficient to strongly increase the concentration of gases, the effect of heating is observed, which is intensified due to feed-back manifestations. Powerful gas ejections often take place prior to volcanic eruptions and in this connection the processes of cooling and warming can be phase-shifted in time with respect to periods of powerful volcanic eruptions. Pulsations of volcanic activity could have been one of the major causes of climatic changes on the Earth in the past epochs.

THE CLIMATIC IMPACT OF THE VOLCANIC ACTIVITY IN THE PROCESS OF THE EVOLUTION OF MARS

It is of interest to compare the climatic impacts of volcanic activities on the Earth and Mars. In contrast to the Earth, the atmosphere of Mars is more rarefied and mainly consists of CO_2. However, during the volcanic activity the chemical composition of the Martian atmosphere had substantially differed from that of the present day, which could have led to substantial changes of climate on Mars.

In the Martian CO_2 atmosphere with low density and humidity, one could expect a lower value of the greenhouse effect $\Delta T = T_s - T_{eff}$, averaged over the entire planet. At the same time, the diurnal temperature variations due to radiative cooling of the atmosphere and diurnal change of the vertical sensible heat exchange, can be rather great. Specific features of the Martian atmosphere manifested in low atmospheric pressure, in its temperature and humidity, could have been a cause of the strong greenhouse effect of specific components, whose temporal trends of content could have been of either cyclic or sporadic character. These factors also include the Martian dust storms and volcanic activity in the process of the atmosphere's evolution.

Latitudinal variations of the vertical temperature profiles in the Martian atmosphere cause an intensive atmospheric circulation, followed by phase transformations of carbon dioxide, water vapour, and by dust storms. During heavy dust leadings of the atmosphere the radiative regime of the planet changes. A strong heating of the atmosphere at the expense of solar radiation absorption by aerosols, and a decrease of the surface temperature - these are the main climatic consequences of dust storms, which are verified not only by Mariner-9 and Viking-1, 2 measurements, but also by results of numerical modelling.

Note that the shortwave radiation absorption by aerosols favours the formation of vertical eddy fluxes in the upper and middle layers of the dust cloud which prevent dust particles from sedimentation. At a planetary surface albedo A = 0.21 the dust aerosol with a single scattering albedo $\tilde{\omega} \geqslant 0.9$ always raises the planetary albedo, and consequently, lowers the effective temperature (the thicker the dust cloud, the lower the temperature). The solution of the problem of radiative heat exchange, in the 1-D approximation, has led to the conclusion about a decrease of the surface temperature with a dust load of the atmosphere increased to an optical thickness of $\tau_a \approx 1.5$.

As the dust load of the atmosphere further grows, the surface temperature slowly increases at the expense of prevailing greenhouse effect of aerosol, which screens the thermal emission of middle layers of the aerosol cloud.

Figure 8 shows vertical temperature profiles calculated for the Martian atmosphere, whose chemical composition and density correspond

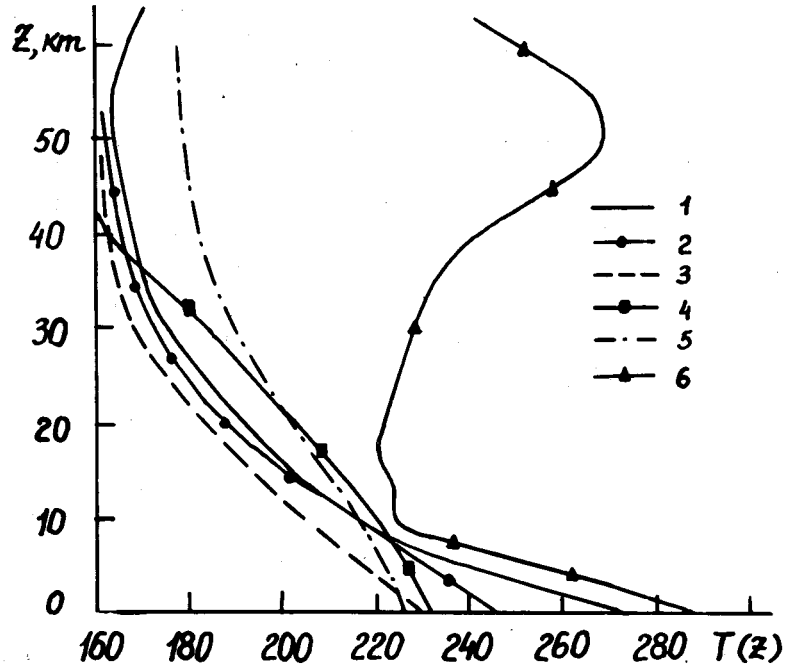

Fig. 8. Vertical temperature profiles T(z) for different meteorological conditions on Mars (curves 1-5); 6 - the mean global vertical temperature profile calculated for the Earth.

to those of the present day. Curve 1 is obtained for the equatorial belt and determines the maximum possible daily mean temperature of the planet for its albedo $\delta = 0.2$, the optical thickness of dust aerosols $\tau_a = 0.1$ (at $\lambda = 0.55\,\mu m$), relative atmospheric humidity $f = 100\%$, and pressure $P_s = 10$ mbar.

Curve 2 corresponds to the same conditions, but for a mean global atmosphere. Curve 3 represents the most probable mean global temperature profile at the atmospheric humidity $f = 0.5$, aerosol optical thickness $\tau_a = 0.55$, pressure $P_s = 6.5$ mbar, and it corresponds to a value of the critical temperature lapse rate $\partial T/\partial z = -2.6\ km^{-1}$. This temperature profile leads to a mean global radiative temperature $T_r = 220K$.

Curves 4, 5 represent the vertical temperature profiles for the near-equatorial region and for the mean global Martian atmosphere, in conditions of a dust storm, with an optical thickness of the dust cloud $\tau_a = 1.0$. Even the warmest area of Mars is characterized by a mean diurnal atmospheric temperature lower than the mean global temperature of the Earth shown by curve 6 in Fig. 8. The greenhouse effect of the Martian atmosphere averages about 10K for the most probable model of the Martian atmosphere.

It is of interest to consider the effect of the Martian atmosphere on the greenhouse effect and temperature of the Martian surface, when the density of the atmosphere and its chemical composition had changed in the process of the evolution of the planet. Of particular interest is the impact of volcanic activity on the climate of Mars.

Clark and Baird (1979) noted that the Martian lava, as to its properties, resembles the basalt lava of the Earth, whose outgassing had been followed by release of a great amount of SO_2 and H_2S (the mixing ratio of sulphur compounds constitutes about 700 ppm). The concentration of sulphur compounds during the outgassing of the Martian lava, should be higher due to more intensive outgassing in conditions of low pressures near the Martian surface.

We assume the mixing ratio of sulphur compounds to be 1000 ppm. The life-time of SO_2 for the present day Martian atmosphere constitutes about $3.9 \cdot 10^3$ days (in the terrestrial atmosphere the life-time of SO_2 is about 110 days). In still earlier periods the pressure and temperature

near the Mars surface could have been higher. However, the life-time of SO_2 had always been long, which appeared to be a cause of the accumulation of a considerable amount of SO_2 in the Martian atmosphere during volcanic eruptions.

During volcanic eruptions a great amount of volcanic ashes and water vapor had been injected to the atmosphere. The latter had favoured the formation of clouds of H_2SO_4-water solutions. The velocity of particles' sedimentation depends on their size, and the time of sedimentation on the surface rapidly decreases with growing size of particles. For instance, particles with a size of 5 μm fall out during 30 days, and 1 μm particles during four years. Since the time of formation of the stratospheric sulphate aerosol on Mars constitutes about two Martian years, the long life-time in conditions of the Martian atmosphere is only possible for submicron aerosols. The consideration of the Martian atmospheric circulation suggests the conclusion that during the formation of submicron particles, the total mixing of aerosols takes place both within the Northern and Southern hemispheres on Mars. Thus, the Martian sulphate aerosol during the volcanic activity is a global-scale phenomenon, substantially affecting the climate on Mars.

The climatic impact of the greenhouse effect on Mars was calculated by Kondratyev, Moskalenko, Parzhin (1981, 1983) in approximation of the radiative-convective equilibrium. The mean-global surface albedo was assumed to be constant and was estimated from the spectral albedo of Mars considered by Moroz (1978).

Major characteristic features of the radiative heat exchange in the atmosphere of Mars for the period of volcanic activity are determined by the following processes:

1. The strong absorption of the shortwave radiation by the atmospheric SO_2 in the wavelength range 0.2-0.4 μm leads to a decrease of the planetary albedo and to the formation of a temperature inversion in the upper atmospheric layers.

2. The formation of clouds from particles of H_2SO_4 water solutions promotes the growth of the planetary albedo and the intensification of the greenhouse effect at the expense of the longwave radiation absorption in the bands of H_2SO_4 water solution.

3. The strong IR SO_2 bands intensify the greenhouse effect in the atmosphere and favour an increase of the temperature of the atmosphere and of the planetary surface.

Mean global Martian surface temperatures as a function of surface pressure, P_S, are listed in Table 2. The atmosphere of Mars is assumed to consist of CO_2, SO_2, and water vapour ($P_{SO_2} = P_{CO_2} \cdot 10^{-3}$).

The vertical pressure profile and the albedo were calculated. The surface albedo was $A_S = 0.19$, and the atmospheric humidity did not exceed $r = 0.5$. When the surface temperature of the planet grows due to the SO_2 greenhouse effect, the moisture content in the atmosphere increases. As a result, the absorption of the thermal emission from the planetary surface and lower troposphere by its upper layers increases, and the greenhouse effect is intensified. SO_2 substantially influences the atmospheric greenhouse effect. Rain- and snowfall become possible even at relatively low pressures near the planetary surface $P_S \approx 0.05$-0.1 atm. The accumulation of SO_2 in great amounts shifts this level toward still lower pressures. During the volcanic activity SO_2 had played the decisive role in formation of climate on Mars, governing the radiative regime of the atmosphere and regulating the climate on the planet.

Table 2

Mean temperature, T_S, near the Martian surface as a function of $P_S(CO_2)$

$P(CO_2)$	δ	$W_{\perp}(H_2)$, cm	T_S, K	T_S^*, K
0.0065	0.205	$1 \cdot 10^{-2}$	238	230
0.01	0.22	$5 \cdot 10^{-5}$	245	233
0.25	0.235	0.15	254	238
0.05	0.25	0.25	263	244
0.1	0.27	0.4	272	252
0.25	0.29	1.0	285	268

Note: $W_{\perp}(H_2O)$ is the water vapour content in the vertical column on Mars; T_S^* is the surface temperature in the absence of SO_2 in the Martian atmosphere.

Periodic variations in the volcanic activity on Mars could have been a cause of considerable temporal changes of its climate.

If the Martian dust clouds lead to the anti-greenhouse effect and lower the temperature of the planetary surface, the effect of volcanoes on the atmosphere in earlier periods of Mars' evolution had created the greenhouse effect and cloud have been a powerful factor of warming on Mars. A hypothesis of a denser Martian atmosphere in the presence of powerful volcanic gas ejections permits to explain a warmer and more humid climate of Mars at still earlier stages of its evolution. Note that volcanic high altitude ejections of water vapour had increased the efficiency of photodissociation of water vapour molecules, which had caused the growth of the ON-radical concentration. This had led to a more intensive absorption of shortwave radiation by the atmospheric hydroxyl in the near UV region and decreased the planetary albedo. The latter could have been an additional factor of warming on Mars during an intensive volcanic activity.

A considerable reduction of volcanic activity resulted in strong cooling of the planet. Upon evaporation, the Martian water partially had dissociated and partially had been accumulated in the form of ice sheets near the poles. As a result of interaction with surface minerals, acid waters had got free of sulphur, which had enriched surface minerals, creating a high concentration of S in them. An increased concentration of sulphur in the elemental composition of the Martian surface, measured from Vikings, confirmed the above mentioned mechanisms for climate changes on Mars.

It is more likely that the warm Martian climate of past epochs had been determined by the presence of SO_2 in the Martian atmosphere but not by a strong burst of solar activity. A broad variety of Martian landscapes had been caused by "river" and "sea" erosive processes and is a direct consequence of the greenhouse effect of the atmosphere with another chemical composition as compared to that of our days. Among other minor components which could have significantly affect the past climate on Mars, were NH_3, CH_4, and NO_2. NH_3 produces very strong greenhouse effect at the expense of absorption of the long- and shortwave radiation. The effect of NO_2 is determined by strong absorption of the shortwave solar radiation and by narrow but intensive vibrational - rotational bands, creating a substantial greenhouse effect.

As a result of tectonic and volcanic activities, the surface of Mars could have obtained a great amount of water. It is not excluded that a

considerable part of the Mars water body had been buried under sand and is, therefore, inaccessible for detection by conventional observational means.

BIBLIOGRAPHY

BARTH, C. A. *et al.*, 1982. Solar mesosphere explorer measurements of El Chichón volcanic cloud. *Bull. Amer. Meteorol. Soc., 63,* 11, 1314 pp.

BORISENKOV, E. P., O. G. VAKHMISTROVA, K. YA. KONDRATYEV, N. I. MOSKALENKO and S. L. HESS, 1981. Climate on planets. Leningrad, Gidrometeoizdat, 95 pp.

CLARK, B. C. and A. K. BAIRD, 1979. Is the Martian lithosphere sulphur rich? *J. Geophys. Res., 84,* B14, 8395-8403.

DEIRMENDJIAN, D., 1971. Scattering electromagnetic emission by spherical particles. Moscow, "Mir" Publ., 165 pp.

JOHN, B., 1982. Winters of our planet. Moscow, "Mir" Publ., 333 pp.

HART, M. A., 1978. The evolution of the atmosphere of the Earth. *Icarus, 33,* 1, 23-39.

KAYUMOVA, G. V., N. I. MOSKALENKO and S. N. PARZHIN, 1979. An atlas of parameters of the spectral absorption lines for atmospheric CO, NO, HCl. *In:* "Abstracts of papers for the 5th All-Union Symp. on the Propagation of the Laser Emission in the Atmosphere".

KONDRATYEV, K. YA., N. I. MOSKALENKO and V. F. TERZI, 1977. Radiative cooling in the atmospheres of Mars, Venus, and Jupiter. *Doklady AN SSSR, 263,* 6, 1334-1337.

KONDRATYEV, K. YA. and N. I. MOSKALENKO, 1979. The greenhouse effect of the planetary atmospheres. *Astronomicheski Vestnik, 8,* 3, 129-143.

KONDRATYEV, K. YA. and N. I. MOSKALENKO, 1980. The evolution of the atmosphere and the greenhouse effect. *Izvestia AN SSSR., FAO, 16,* 11, 1151-1162.

KONDRATYEV, K. YA. and N. I. MOSKALENKO, 1980. The radiative heat exchange in the atmosphere of Mars and the greenhouse effect. *Doklady AN SSSR, 255,* 1, 64-66.

KONDRATYEV, K. YA. and G. S. HUNT, 1981. Weather and climate of planets. Pergamon Press, Oxford, 755 pp.

KONDRATYEV, K. YA., N. I. MOSKALENKO and S. N. PARZHIN, 1981. The greenhouse effect of the Martian atmosphere during an intensive volcanic activity. *Doklady AN SSSR, 266,* 1, 55-58.

KONDRATYEV, N. YA. and N. I. MOSKALENKO, 1981. The greenhouse effect of planetary atmospheres. *Nuovo Cimento, 4C,* 6, 698-735.

KONDRATYEV, K. YA., N. I. MOSKALENKO and S. N. PARZHIN, 1983. Optical properties of the Martian atmosphere and radiative heat exchange. *Adv. Space Res., 2,* 10, 39-42.

KONDRATYEV, K. YA., N. I. MOSKALENKO and V. P. TERZI, 1981. A closed modelling of the optical characteristics of the atmospheric aerosol. *Doklady AN SSSR, 253,* 6, 1354-1356.

KONDRATYEV, K. YA., N. I. MOSKALENKO, V. F. TERZI and S. YA. SKVORTSOVA, 1981. Modelling the optical characteristics of atmospheric aerosols. *In:* "GARP: Aerosol and Climate". Leningrad, *Gidrometeoizdat, 1,* 130-153.

KONDRATYEV, K. YA. and N. I. MOSKALENKO, 1983. Key problems in studies of terrestrial planets (The greenhouse effect of planetary atmospheres). *Adv. in Sci. & Technol., Ser. Studies in Space, 19,* 157 pp.

KONDRATYEV, K. YA., N. I. MOSKALENKO and D. V. POZDNYAKOV, 1983. Atmospheric aerosols. Leningrad, *Gidrometeoizdat,* 224 p.

KONDRATYEV, K. YA., 1983. The El Chichón volcano eruption: the observed and possible impacts on the atmosphere. Moscow, VINITI, Preprint No.44, AN SSSR, 54 pp.

LABITZKE, K., N. NAUJOKAT and M. P. McCORMICK, 1982. Temperature effects on stratosphere of the April 4, 1982 eruption of El Chichón. México, Preprint Meteorol. Inst., Free Univ., Berlin, 6 pp.

LAMB, N. N., 1977. Climate: Present, Past, and Future. Vol. II, Climatic history and future. London, Methuen, New York, Barnes and Noble, 835 pp.

MAROV, M. YA., 1981. Planets of the solar system. Moscow, "Nauka" Publ. 256 pp.

McCLATCHEY, R. R. (Ed.), 1973. APCRL atmospheric absorption line parameters compilation. Environ. Res. Paper, 434, 78 pp.

MOROZ, V. I., 1978. Physics of the planet Mars. Moscow, "Nauka" Publ.

MORSS, D. A. and W. R. KUHN, 1978. Paleoatmospheric temperature structure. *Icarus, 33,* 1, 40-49.

MOSKALENKO, N. I., 1969. Experimental integral absorption functions for the bands of H_2O, CO_2, N_2O, CH_4, CO, NO vapours. *Izvestia AN SSSR, FAO, 5,* 9, 962-966.

MOSKALENKO, N. I., 1975. Specific features of the spectral and spatial distributions of the thermal emission field in the atmosphere of Mars. *Izvestia AN SSSR, FAO, 11,* 8, 836-844.

MOSKALENKO, N. I. and A. R. ZAKIROVA, 1972. The calculation of the spectral, angular, and vertical distributions of the thermal emission field of the atmosphere and surface of the Earth. *Izvestia AN SSSR, FAO, 8,* 8, 828-842.

MOSKALENKO, N. I. and O. V. ZOTOV, 1977. Latest experimental studies and specifications of the CO_2 spectral transmission functions: the line parameters. *Izvestia AN SSSR, FAO, 13,* 5, 488-498.

MOSKALENKO, N. I., YU. A. ILYIN and S. N. PARZHIN, 1978. Continuum and pressure-induced absorptions in the spectra of CO_2 and water vapour. *In:* "Abstracts of papers for the 5th All-Union Meeting on Molecular Spectroscopy of High and Super-High Resolution". Novosibirsk, p.187-191.

MOSKALENKO, N. I., V. F. TERZI, S. N. PARZHIN, V. T. PUSHKIN and R. S. SADYKOV, 1978. Studies of the sulphureous gas absorption spectra in the IR spectral region. *In:* "Abstracts of papers for the 11th All-Union Meeting on Actinometry". Tallin, Part 6, p.51-56.

MOSKALENKO, N. I., V. F. TERZI and S. YA. SKVORTSOVA, 1981. The optical characteristics of aerosol formations. *In:* "GARP. Aerosol and Climate". Leningrad, *Gidrometeoizdat, 1,* 154-165.

MOSKALENKO, N. I. and F. S. YAKUPOVA, 1978. A solution for the problems of radiation transfer in the atmosphere by computer-modelling. *In:* "Abstracts of papers for the IV All-Union Meeting on Molecular Spectroscopy of High and Super-High Resolution". Novosibirsk, p. 178-182.

NEWELL, R. E. and A. DEEPAK, 1982. Mount St. Helens eruptions of 1980. Atmospheric effects and potential climatic impact. NASA SP-458, Washington, D. C., 119 pp.